Computation of Schottky barriers in semiconducting ferroelectric barium titanate in reducing atmospheres

Ahmed Amin
Texas Instruments Incorporated, Attleboro, Massachusetts 02703
(Received 4 June 1993; revised manuscript received 21 September 1993)

The time and temperature dependencies of the double Schottky barriers in semiconducting ferroelectric barium titanate ($BaTiO_3$) in the presence of a reducing or an oxidizing atmosphere are considered. Numerical computations of the local variation of barrier heights as a function of time and temperature are presented for both bulk and thin films. Experimental observations and theoretical results are analyzed for donor-doped semiconducting polycrystalline $BaTiO_3$.

INTRODUCTION

Experimental observations of the dependence of the room-temperature resistivity and the magnitude of the positive temperature coefficient (PTC) of the resistivity anomaly of semiconducting donor-doped $BaTiO_3$ polycrystals in reducing or oxidizing atmospheres are well documented in the literature.[1-4] It has been observed that the magnitude of the PTC anomaly can be drastically decreased or even eliminated in reducing environments such as carbon monoxide. Conversely, oxidizing atmospheres (e.g., oxygen) restore this anomaly. The observed steady-state and transient responses[1] of semiconducting $BaTiO_3$ polycrystals under the influence of carbon monoxide and oxygen are displayed in Figs. 1 and 2, respectively.

In this work we will seek to develop a theoretical framework which could explain "semiquantitatively" the phenomena exhibited by Figs. 1 and 2. The treatment is based on the diffusion-reaction theory in porous media, the double Schottky model of the grain boundary barriers, and the Landau-Ginzburg-Devonshire phenomenology of ferroelectric phase transition in $BaTiO_3$. We hope this analysis will provide further insights into the PTC phenomenon and its stability.

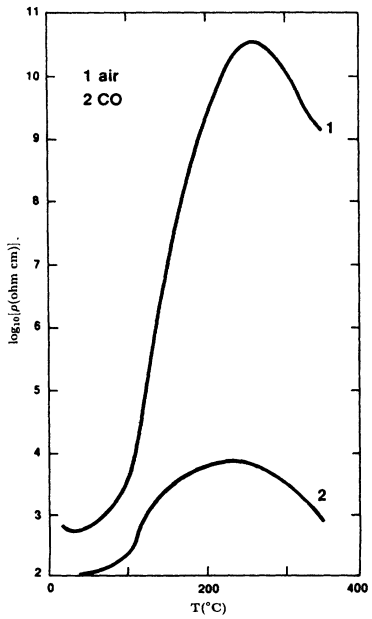

FIG. 1. Resistivity vs temperature characteristics of a semiconducting $Ba_{0.998}Sb_{0.002}TiO_3$ PTC composition upon heating (1) in air and (2) in CO (Ref. 1).

Semiconducting donor-doped polycrystalline barium titanate $BaTiO_3$ exhibits an anomalous increase in resistivity[5,6] known as the positive temperature coefficient of resistivity above the ferroelectric Curie temperature T_C. No appreciable anomaly was observed in the doped single crystal.[7] The semiconducting properties are produced by (i) doping with a trivalent element such as La^{3+} or Y^{3+} which substitutes for Ba^{2+} on the cubo-octahedral site, or (ii) doping with a pentavalent element such as Nb^{5+} or Sb^{5+} which substitutes for titanium. In this manner free electrons are generated in the titanium $3d$ conduction band through the formation of a Ti^{4+}: Ti^{3+} complex: $(Ba^{2+}_{1-x}Ln_x)(Ti^{4+}_{1-x}Ti^{3+}_x)O_3$. The dopant concentration is usually less than 0.3 at %.

Below the ferroelectric-paraelectric phase transition temperature T_C, Schottky barriers between the semiconducting $BaTiO_3$ grains are neutralized by the spontaneous polarization P_s associated with the ferroelectric phase transition.[8] Above T_C the barrier height increases rapidly with temperature due to the disappearance of P_s

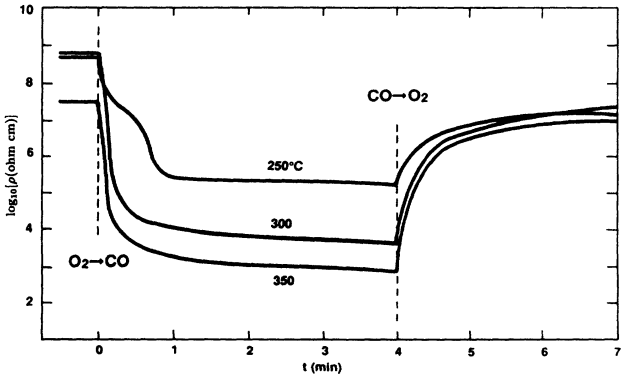

FIG. 2. Transient response isotherms (Ref. 1).

and the decrease of the paraelectric state dielectric constant (Curie-Weiss law). Semiconducting $BaTiO_3$ (PTC) elements are commercially available with Curie temperature ranges from $-80\,^{\circ}C$ to $300\,^{\circ}C$ and room-temperature resistivities between 10 and 20 Ω cm with eight orders of magnitude change in the resistivity at T_C. They are used in a variety of applications.[9,10]

The existence of surface acceptor states is a necessary condition for barrier formation. It is generally believed that the grain boundary (back-to-back) Schottky barriers are due to chemisorbed oxygen or halogen.[8] Acceptor states are generated at the grain boundary through oxygen adsorption and diffusion during the high-temperature sintering of $BaTiO_3$. Conduction electrons become trapped in the interfacial states leading to the formation of depletion layers. Since a large amount of charge is trapped at the grain boundary, a high capacitance is expected. Formation electrical junctions with good PTC properties require values of surface-state densities ranging from $2\times10^{18}/m^2$ to $4\times10^{18}/m^2$.

The depletion region between the semiconducting grains in $BaTiO_3$ has been observed by several imaging techniques.[11] Other lattice defect models have been proposed for the surface acceptor states.[12–15] These include oxidized impurities which are expected to provide fairly deep traps, a gradient of Ba vacancies, and a gradient of Ti vacancies, however, their nature still is controversial. Whatever their source may be (chemisorbed oxygen, or hole compensated acceptor-doped skin), surface states must exist for grain boundary barriers to occur.

The barrier layer potential in semiconducting donor-doped $BaTiO_3$, in addition to its temperature dependence, is also a function of the electric[15,16] and elastic[17–19] boundaries and of the size of the semiconducting grains. The decrease of the magnitude of the PTC anomaly with dc field bias is attributed to Schottky emission across the barriers. Barriers can also be raised or lowered depending upon the nature of the elastic boundaries. Hydrostatic pressure, for example, raises the barrier potential, whereas uniaxial stresses would either raise or lower the barrier depending upon the sign of the electrostriction tensor components in the Landau-Ginzburg-Devonshire free energy density function.[18,19]

BULK POLYCRYSTALS

The grain boundary barrier of a semiconducting polycrystalline (PTC) $BaTiO_3$ is modeled as a strong-depletion–slight-inversion, back-to-back Schottky barrier.[6] The expression for the static, quiescent condition (zero current) Schottky-Heywang barrier height Φ is obtained by solving Poisson's equation under the assumption that barium titanate is a linear and isotropic dielectric, a valid assumption above T_C.

$$\Phi = e^2 n_s^2 / 8\epsilon\epsilon_0 N_d \ , \tag{1}$$

where e is the electronic charge, n_s the net concentration of ionized surface acceptor states, ϵ the dielectric constant, ϵ_0 the free space permittivity (8.854×10^{-12} F/m), and N_d the donor concentration per unit volume.

Above the Curie temperature T_C, the Curie-Weiss law is obeyed and the dielectric constant for $BaTiO_3$ is given by

$$\epsilon = C/(T-T_0) \ , \tag{2}$$

where C is the Curie-Weiss constant and T_0 the extrapolated Curie-Weiss temperature. According to the Landau-Ginzburg-Devonshire theory of a proper ferroelectric derived from a prototypic symmetry group $Pm3m$ (e.g., $BaTiO_3$), the single-domain paraelectric state dielectric stiffness (dielectric reciprocal susceptibility) χ^{-1} is given by

$$\chi^{-1} = 2\alpha_1\epsilon_0 \ , \tag{3}$$

where α_1 is the tensor coefficient of the second-order polarization term in the free energy density function (described under thin film). For high permittivity solids such as $BaTiO_3$, it is valid to assume that $\chi \approx \epsilon$. Thus

$$\alpha_1 = (1/2\epsilon_0 C)(T-T_0) = \beta(T-T_0) \ , \tag{4}$$

where $\beta = 1/(2\epsilon_0 C)$. The expression for barrier height under the conditions of zero applied stress and field is obtained by combining Eqs. (1)–(3) to yield,

$$\Phi = (\beta e^2 n_s^2 / 4N_d)(T-T_0) \ . \tag{5}$$

The surface acceptor states, according to Heywang's model are assumed to lie at one fixed energy level E_s, well below the Fermi level E_f (fully occupied), and the donor levels are sufficiently close to the conduction band (fully ionized). The net concentration of the ionized surface acceptor states n_s is given by

$$n_s = N_s / \{1+\exp[(E_F+\Phi-E_s)/kT]\} \ , \tag{6}$$

where N_s is the density of the surface acceptor states, the occupation probability F (Fermi-Dirac) is given by

$$F = 1/\{1+\exp[(E_F+\Phi-E_s)/kT]\} \ , \tag{7}$$

where k is Boltzmann's constant. The position of the Fermi level E_F is determined from the effective density of states in the conduction band N_c and the donor concentration N_d by

$$E_F = kT \ln(N_c/N_d) \ , \tag{8}$$

where $N_c = 2(2\pi m_e^* kT/h^2)^{3/2}$, with m_e^* being the electron effective mass, and h Planck's constant. Equation (8) is a valid approximation for $E_F < -kT$, i.e., for $N_d < 2N_C$. The grain boundary resistivity ρ of $BaTiO_3$ is written as

$$\rho = \rho_0 \exp(\Phi/kT) \ . \tag{9}$$

Substituting from Eq. (8) into Eq. (6), the transcendental equations (5) and (6) can be solved iteratively to give the barrier height Φ and the occupation probability of the surface acceptor states as a function of temperature.

The time dependence of the Schottky barriers in the presence of a reducing or an oxidizing atmosphere can be treated as a diffusion reaction phenomenon. The reducing gas species, for example, diffuses into the semiconductor and reacts with the oxygen at the surface states (be-

comes immobilized). This reaction frees the trapped electron which can enter the conduction band of the semiconductor. Consequently, the net concentration of the ionized surface acceptor states n_s, and hence the barrier height Φ, will be a function of the reducing gas species concentration C in the semiconducting $BaTiO_3$ sample at any given time. The form of this function will be discussed next.

We will consider the diffusion-reaction model through a porous medium as treated by Crank.[20] In this model the reducing gas species diffuses within the pores of the semiconductor element and becomes immobilized very rapidly, i.e., the chemical reaction with the oxygen at the surface states is much faster compared with the diffusion. Therefore diffusion is the rate controlling process. In this manner, local equilibrium can be assumed to exist between the free and immobilized components of the diffusing species. The concentration S of the immobilized species is directly proportional to the concentration C of the species free to diffuse, i.e.,

$$S=RC \ , \tag{10}$$

and the diffusion adsorption equation becomes

$$D\nabla^2 C-\frac{\partial S}{\partial t}=\frac{\partial C}{\partial t} \ , \tag{11}$$

where D is the diffusion coefficient which is assumed to be isotropic and independent of concentration. Substituting from Eq. (10) into Eq. (11), we get

$$\frac{D}{(R+1)}\nabla^2 C=\frac{\partial C}{\partial t} \ . \tag{12}$$

Equation (12) shows that the overall diffusion process is slowed down by a factor $(R+1)$ as a result of adsorption-reaction process. We may consider $D_e=D/(R+1)$ as being an effective diffusion coefficient. Thus, Eq. (12) becomes

$$D_e\nabla^2 C=\frac{\partial C}{\partial t} \ . \tag{13}$$

If the linear relation [Eq. (10)] holds, solutions of the above differential equation with reaction, for given initial and boundary conditions, are the same for the corresponding problem in simple diffusion, except the effective diffusion coefficient D_e is to be used. For a rectangular parallelepiped with constant surface concentration C_0 and with dimensions $2a$, $2b$, and $2c$ such that $-a<x<a$, $-b<y<b$, and $-c<z<c$, the solution of the diffusion equation subject to the initial and boundary conditions $C=0$ at time $t=0$ at all points of the medium and $C=C_0$ at $t>0$ at all points of the surface is reduced to the one-dimensional case (for $a \ll b,c$),

$$c(x,t)=C/C_0=1-(4/\pi)\sum_{l=0}^{\infty}[(-1)^l/(2l+1)] \times\cos(2l+1)(\pi x/2a) \times\exp(-t\alpha_1) \ , \tag{14}$$

where

$$\alpha_1=(\pi^2 D/4)(2l+1/a)^2 \ . \tag{15}$$

Equation (14) is identical to that of a linear heat flow in a solid bounded by two parallel planes kept at a constant temperature or insulated. Carslaw and Jaeger.[21] Numerical computation of $c(x,t)$ for different values of the normalized distance (x/a) and normalized time t (expressed as fractions of the diffusion time constant a^2/D) is shown in Fig. 3.

Let us write the following expression for the uncompensated net concentration of acceptor surface states n_s,

$$n_s=N_s F[1-c(x,t)] \ , \tag{16}$$

where F and $c(x,t)$ are given by Eqs. (7) and (14), respectively. For oxidizing atmospheres the negative sign in Eq. (16) is replaced by a positive one. Thus, in order to determine the temperature and time dependence of the Schottky barriers $\Phi(T,t)$ and the occupation probability of the surface acceptor states $F(T,t)$, we need to solve the following transcendental equations with the appropriate parameters written between ( ):

$$\Phi(T,t)=(\beta e^2 n_s^2/4N_d)(T-T_0) \ , \tag{5'}$$

$$n_s=N_s F(T,t)[1-c(x,t)] \ , \tag{16'}$$

$$F(T,t)=1/(1+\exp\{[E_F+\Phi(T,t)-E_s]/kT\}) \ . \tag{7'}$$

Hall measurements[5,22] on semiconducting PTC samples revealed low electron mobility ($\approx 10^{-2}$ $cm^2 v^{-1} s^{-1}$), so that the conduction band is most probably narrow. Hence, the density of the states in the conduction band N_c will be the number of Ti ions per unit volume ($\approx 1.6\times 10^{28}$ m^{-3}), just as is usually found for transition metal oxides with completely localized electron states.[8] This was further confirmed by thermoelectric power and Hall measurements on samples whose barrier layers were destroyed by reduction,[23] and small polaron formation whose mobility is enhanced by successive hops.[24,25] Other physical constants for $BaTiO_3$ which were used in the numerical analysis are well documented in the literature[8,26] and are as follows: $N_d=10^{25}$ m^{-3}, $N_s=2\times 10^{18}$ m^{-2}, $E_s=1.442\times 10^{-19}$ CV, $C=1.7\times 10^5$ K, $T_0=381$ K.

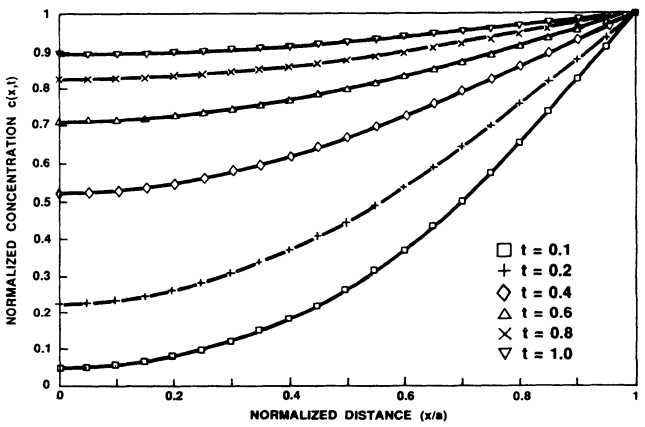

FIG. 3. Computed concentration profiles vs distance at different times (t) taken as fractions of the diffusion time constant (a^2/D).

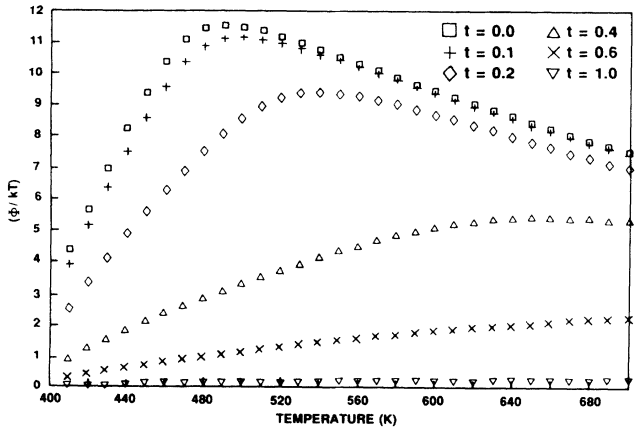

FIG. 4. Computed (Φ/kT) vs temperature at different times (t) taken as fractions of the diffusion time constant, $x/a=0.0$.

Equations (5′) and (16′) are solved iteratively using the bisection method to yield the barrier height $\Phi(T,t)$ and the occupation probability of the surface acceptor states as a function of temperature and time. The temperature and time dependencies of Φ/kT and the occupation probability of the surface acceptor states are shown in Figs. 4 and 5 respectively, for $x/a=0.0$. A graphical representation of Φ/kT for an element coordinate $x/a=0.5$ is shown in Figs. 6. Figure 7 illustrates the manner in which the barrier height varies with time under isothermal conditions.

Model computations (Figs. 4 and 7) of the temperature and time dependencies of the grain boundary barriers in semiconducting $BaTiO_3$ polycrystals agree semiquantitatively with the experimental observations displayed in Figs. 1 and 2. The experimental resistivity curves displayed in Fig. 1 show an interesting feature of the steady-state PTC response after exposure to CO. That is, the PTC maximum is not only lowered relative to that in air but is also flatter. A plausible explanation would be an energetic distribution of the surface acceptor states after exposure to CO, i.e., they occupy a range of energy states below the Fermi level, rather than a single degen-

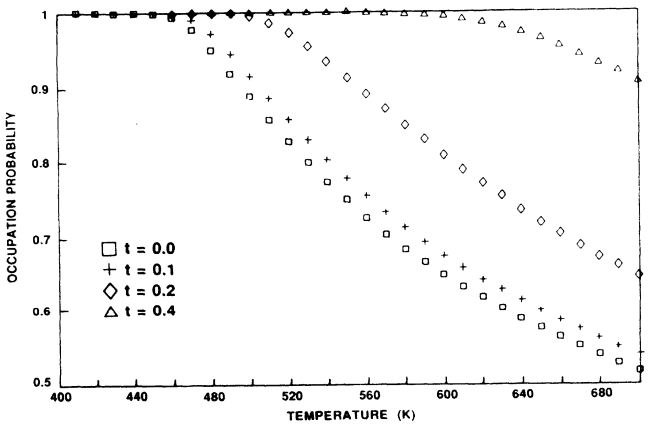

FIG. 5. Occupation probability of the surface acceptor states vs temperature at different times (t) taken as fractions of the diffusion time constant, $x/a=0.0$.

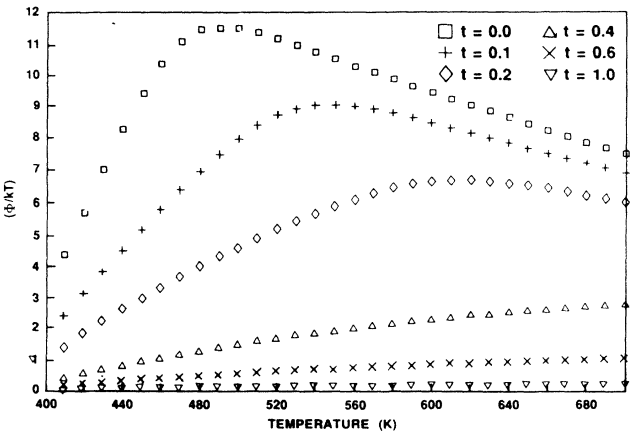

FIG. 6. Computed (Φ/kT) vs temperature at different times (t) taken as fraction of the diffusion time constant, $x/a=0.5$.

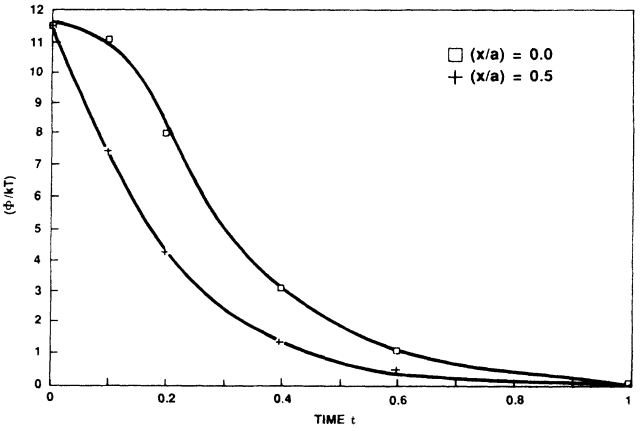

FIG. 7. Computed isothermal transient response for $x/a=0.0$ and 0.5 at 490 K (theoretical PTC maximum).

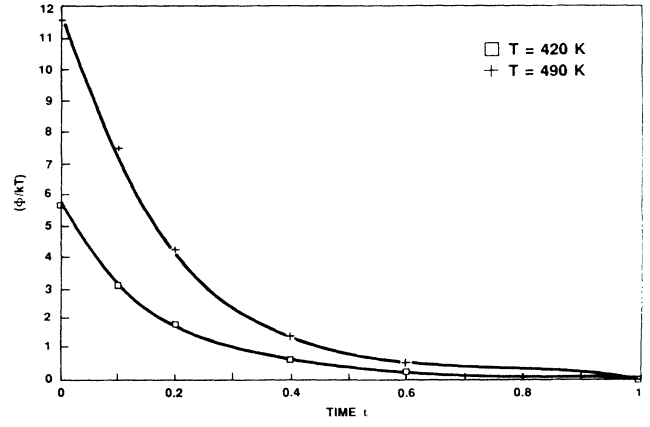

FIG. 8. Computed transient isotherm at 420 K (PTC region), along with the response at PTC maximum for comparison $(x/a=0.5)$.

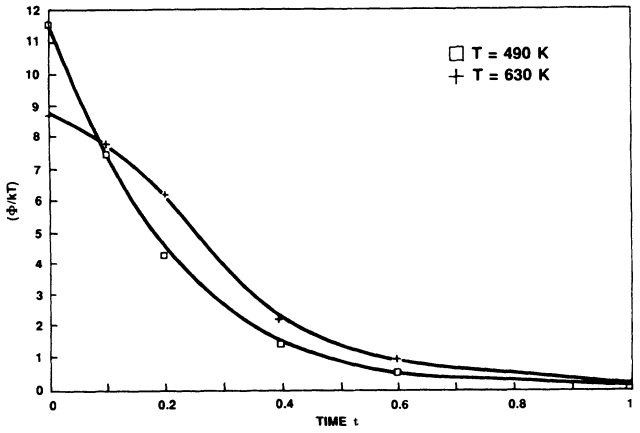

FIG. 9. Computed transient isotherm at 630 K (NTC region), along with the response at PTC maximum for comparison ($x/a=0.5$).

erate level E_s.[24] Another possibility is the existence of inhomogeneous stresses at the grain boundaries. The isothermal transient response computed at 490 K (theoretical PTC maximum) displayed in Fig. 7 is in a general agreement with the experimental results (Fig. 2). The manner in which the isothermal transient responses vary with temperature will depend on the location of the operating temperature on the PTC curve. This is illustrated in Figs. 8 and 9, which show the theoretical transient isotherms in the PTC and NTC regions, respectively. Further comments on the experimental and theoretical time and temperature dependencies of the double Schottky barriers in semiconducting $BaTiO_3$ will be given in the discussion section.

THIN FILMS

There has been an increasing interest in recent years in the development of ferroelectric thin films for memory and linear integrated circuit (IC) applications.[27–29] A great deal of effort has been devoted to the deposition of the perovskite family ferroelectrics, particularly $BaTiO_3$, (Ba, Sr)TiO_3, $PbTiO_3$, and (Pb, Zr)TiO_3 on a variety of substrates. Film deposition techniques range from sputtering, metallo-organic chemical vapor deposition, laser ablation, etc., to sol-gel, pyrolysis, spin coating, etc. The most commonly used substrates are Si, MgO, sapphire, and to a lesser extent quartz. Pulsed excimer laser deposition of La^3-doped semiconducting $BaTiO_3$ on p-type Si, quartz, glass, and alumina substrates has been described in a recent article.[30]

In ferroelectric thin films, additional factors must be considered due to the presence of a stress pattern which could conceivably evolve for a number of reasons, such as thermal expansion mismatch with the substrate, stress relaxation from the lattice, microstructural imperfections, or the film substrate interface.[31] Recent x-ray diffraction measurements[32] on epitaxially grown thin ferroelectric lead titanate $PbTiO_3$ films showed that the tetragonal-cubic phase transition occurred for some films at a temperature $\approx 50\,^{\circ}C$ higher than the single crystal ($\approx 490\,^{\circ}C$). In addition, the films were elongated along the crystallographic c axis compared to pure $PbTiO_3$. Using a phenomenological Landau theory for $PbTiO_3$, the observed shifts in Curie temperature were attributed to a two-dimensional compressive stress pattern.[33]

In ferroelectric polycrystals and thin films, a complete free energy function is particularly valuable, since often the elastic and electric boundary conditions upon the individual crystallites are uncertain. It is frequently not clear whether the "unusual properties" are intrinsic and to be associated with these boundary conditions or are extrinsic and associated with such phenomena as domain and phase boundary motion.

The ferroelectric nature of the grain boundary layer in semiconducting barium titanate makes it possible to use the Landau-Ginzburg-Devonshire phenomenological theory. For many ferroelectric crystals, this formalism gives an excellent semiquantitative description of the dielectric, elastic, and piezoelectric properties when only the lowest-temperature terms are linearly temperature dependent, higher-order terms temperature independent, and often for a very truncated series expansion. For a more accurate description over a wider temperature range, additional higher-order terms, and/or temperature-dependent higher-order coefficients can be included.[34]

Consider the free energy density function for a proper ferroelectric derived from a prototypic symmetry group $Pm3m$. For Brillouin zone center lattice modes, the Landau-Ginzburg-Devonshire free energy density function (thermodynamic potential) may be written as a power series in terms of the order parameter (the dielectric polarization vector) P_i ($i=1,2,3$) as follows:

$$
\begin{aligned}
G=&\alpha_1(P_1^2+P_2^2+P_3^2)+\alpha_{11}(P_1^4+P_2^4+P_3^4)+\alpha_{12}(P_1^2P_2^2+P_2^2P_3^2+P_3^2P_1^2)+\alpha_{111}(P_1^6+P_2^6+P_3^6)\\
&+\alpha_{112}[P_1^4(P_2^2+P_3^2)+P_2^4(P_3^2+P_1^2)+P_3^4(P_1^2+P_2^2)]+\alpha_{123}P_1^2P_2^2P_3^2-1/2s_{11}(X_1^2+X_2^2+X_3^2)\\
&-s_{12}(X_1X_2+X_2X_3+X_3X_1)-1/2s_{44}(X_4^2+X_5^2+X_6^2)-Q_{11}(X_1P_1^2+X_2P_2^2+X_3P_3^2)\\
&-Q_{12}[X_1(P_2^2+P_3^2)+X_2(P_3^2+P_1^2)+X_3(P_1^2+P_2^2)]-Q_{44}(X_4P_2P_3+X_5P_3P_1+X_6P_1P_2)\,,
\end{aligned}
\tag{17}
$$

where α_i, α_{ij}, α_{ijk} (in the reduced tensor notation) are related to the dielectric stiffness (dielectric reciprocal susceptibility) and higher-order stiffness coefficients at constant stress and Q_{11}, Q_{12}, Q_{44} are the electrostriction constants written in polarization notation. In Eq. (17) tensile stresses are denoted by X_1, X_2, X_3, and the shear components by X_4, X_5, X_6, respectively. The expression is complete up to all six power terms in polarization, but contains only first-order terms in electrostrictive and elastic behavior.

The first partial derivatives of the free energy density function with respect to the components of P_i, X_i, and T give the conjugate coordinates, the electric field E_i, the negative of the strain $-x_i$, and the entropy change $-S$, respectively,

$$\frac{\partial G}{\partial P_i}=E_i \ , \tag{18}$$

$$\frac{\partial G}{\partial X_{ij}}=-x_{ij} \ , \tag{19}$$

$$\frac{\partial G}{\partial T}=-S \ . \tag{20}$$

The single domain dielectric stiffness (reciprocal susceptibilities) $1/\chi_{ij}$ is given by the appropriate second partial derivatives.

$$\frac{\partial^2 G}{\partial P_i \partial P_j}=\frac{1}{\chi_{ij}} \ , \tag{21}$$

Equation (17) has two solutions of interest for the stress-free "unclamped" ferroelectric grain boundary layer of semiconducting $BaTiO_3$ PTC polycrystals. The first solution corresponds to the prototypic paraelectric cubic state (symmetry group: $Pm3m$) and the second to the ferroelectric tetragonal state ($P4mm$). These follow.

(i) Paraelectric state ($T>T_C$):

$$P_1^2=P_2^2=P_3^2=0 \ ,$$

$$\chi_{11}=\chi_{22} \ , \quad \chi_{33}=\chi_p \ , \quad \chi_{12}=\chi_{23}=\chi_{31}=0 \ , \tag{22}$$

$$(1/\chi_p)=2\alpha_1\epsilon_o \ , \tag{23}$$

according to the Curie-Weiss law, the dielectric stiffness constant α_1 is given a linear temperature dependence,

$$\alpha_1=(1/2\epsilon_0 C)(T-T_0) \ . \tag{24}$$

(ii) Ferroelectric state ($T<T_c$):

$$P_1^2=P_2^2=0 \ ,$$

and the spontaneous polarization ($P_s=P_3$) is determined from the stability conditions $\partial G/\partial P_3=E_3=0$, therefore

$$P_3^2=\{-\alpha_{11}+[(\alpha_{11})^2-3\alpha_1\alpha_{111}]^{0.5}\}/3\alpha_{111} \ , \tag{25}$$

$$\chi_{11}=\chi_{22}\neq\chi_{33} \ , \quad \chi_{12}=\chi_{23}=\chi_{31}=0 \ , \tag{26}$$

$$(1/\chi_{33})=(2\alpha_1+12\alpha_{11}P_3^2+30\alpha_{111}P_3^4)\epsilon_0 \ , \tag{27}$$

$$(1/\chi_{11})=(2\alpha_1+2\alpha_{12}P_3^2+2\alpha_{112}P_3^4)\epsilon_0 \ . \tag{28}$$

The expressions for the barrier heights under different thermal and elastic boundary conditions have been derived from the free energy density function.[18,19] We summarize below the expressions which are required for the numerical solutions of the barrier heights and the occupation probability of the surface states in the presence of reducing or oxidizing atmospheres, under different thermal and elastic boundaries.

(i) Hydrostatic stress (X_h):

$$\Phi(T,t,X_h)=(\beta e^2 n_s^2/4N_d)[T-(T_0-Q_h\beta^{-1}X_h)] \ , \tag{29}$$

$$F(T,t,X_h)=1/(1+\exp\{[E_F+\Phi(T,t,X_h)-E_s]/kT\}) \ , \tag{30}$$

$$n_s=N_s F(T,t,X_h)[1-c(x,t)] \ , \tag{31}$$

where Q_h ($=Q_{11}+2Q_{12}$) is the hydrostatic electrostriction coefficient.

(ii) Uniaxial stress X_3 perpendicular to the film plane:

$$\Phi(T,t,X_3)=(\beta e^2 n_s^2/4N_d)[T-(T_0-Q_{11}\beta^{-1}X_3)] \ , \tag{32}$$

$$F(T,t,X_3)=1/(1+\exp\{[E_F+\Phi(T,t,X_3)-E_s]/kT\}) \ , \tag{33}$$

$$n_s=N_s F(T,t,X_3)[1-c(x,t)] \ . \tag{34}$$

(iii) Uniaxial stress X_1 in the film plane:

$$\Phi(T,t,X_1)=(\beta e^2 n_s^2/4N_d)[T-(T_0-Q_{12}\beta^{-1}X_1)] \ , \tag{35}$$

$$F(T,t,X_1)=1/(1+\exp\{[E_F+\Phi(T,t,X_1)-E_s]/kT\}) \ , \tag{36}$$

$$n_s=N_s F(T,t,X_1)[1-c(x,t)] \ . \tag{37}$$

(iv) Biaxial stress X_b in the film plane:

$$\Phi(T,t,X_b)=(\beta e^2 n_s^2/4N_d)[T-(T_0-2Q_{12}\beta^{-1}X_b)] \ , \tag{38}$$

$$F(T,t,X_b)=1/(1+\exp\{[E_F+\Phi(T,t,X_b)-E_s]/kT\}) \ , \tag{39}$$

$$n_s=N_s F(T,t,X_b)[1-c(x,t)] \ . \tag{40}$$

A hydrostatic stress or a uniaxial stress oriented normal to the film plane will have the effect of shifting the Curie temperature to a lower value relative to the unstressed state. Nevertheless, a uniaxial or a biaxial stress in the film plane will tend to shift the Curie temperature to a higher value relative to the stress-free state. The electrostriction tensor components Q_{11} and Q_{12} for $BaTiO_3$ have the values 0.1107 and -0.0432 m^4C^{-2}, respectively.[26]

According to Eqs. (38) and (29), respectively, a biaxial

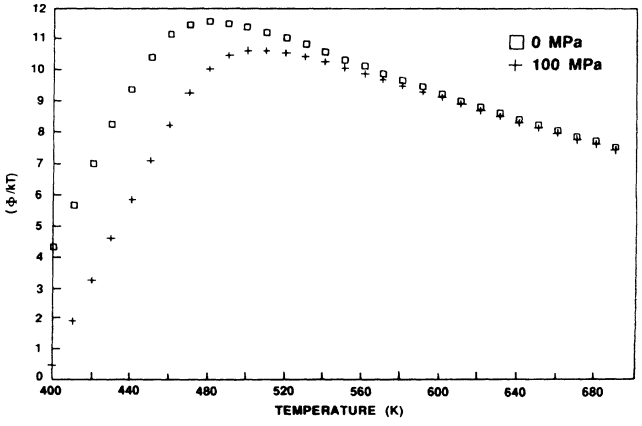

FIG. 10. The effect of a biaxial stress on Φ/kT vs temperature characteristics for thin film semiconducting PTC.

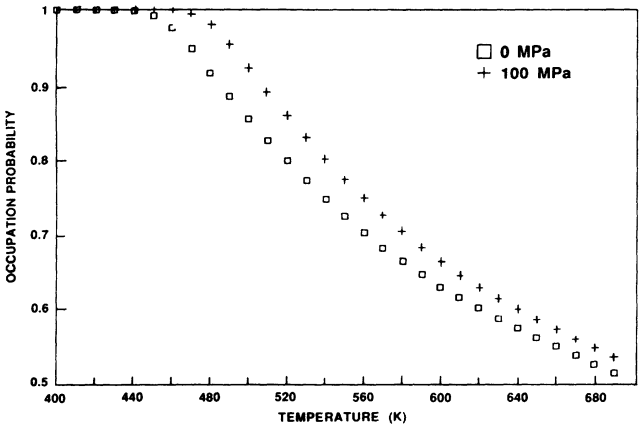

FIG. 11. The influence of a biaxial stress on the occupation probability of the surface acceptor states of thin film semiconducting PTC.

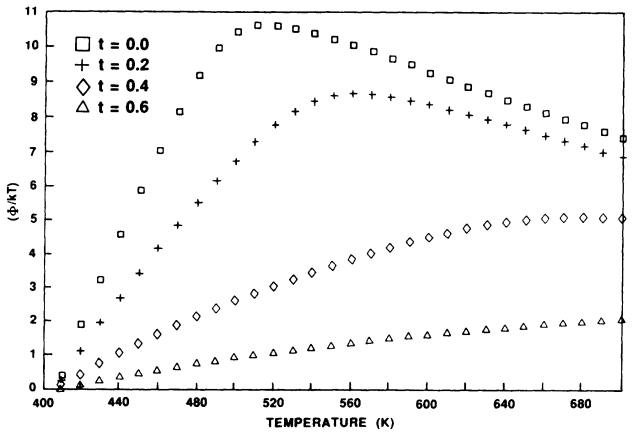

FIG. 12. Variation of (Φ/kT) vs temperature at different times (t), for a thin film semiconducting PTC, $x/a=0.0$.

stress in the film plane will have a much more pronounced effect on the Curie temperature than a hydrostatic one. This is because in ferroelectric perovskites derived from the prototypic symmetry $Pm3m$, the strain is electrostrictively coupled to the order parameter via the electrostriction tensor components Q_{11}, Q_{12}, and Q_{44} [Eq. (17)]. Since for most perovskites, $Q_{11}\approx -2Q_{12}$, and $Q_h=Q_{11}+2Q_{12}$, therefore a large hydrostatic stress would be required to produce the same magnitude of Curie temperature shifts as it would be for a biaxial stress.

Computational results of barrier heights and the occupation probability of the surface states for a biaxially clamped thin film are shown in Figs. 10 and 11. The temperature and time dependence of Φ/kT for thin films are depicted in Fig. 12. Qualitatively they are similar to the corresponding bulk results except they are shifted to a higher temperature as a result of the biaxial stress components in the film plane. Consequently, the isothermal transient response of a thin film will be suppressed relative to that of the bulk with the same composition as shown in Fig. 13. Experimental data on the influence of reducing or oxidizing atmospheres on the resistivity of thin films are unavailable at this time.

DISCUSSION

A semiquantitative treatment has been developed which accounts for the time and temperature dependencies of the double Schottky barriers in semiconducting positive temperature coefficient of resistivity barium titanate in the presence of a reducing or an oxidizing environment. Further refinements of model computation require an accurate knowledge of the nature of surface acceptor states, their density and energetic distribution. In principle, surface-state density can be measured by capacitance—voltage techniques with metal electrodes near the surface or on surface barrier diodes. As pointed out by Miller,[35] the problems of obtaining a clean surface complicated the first technique. On the other hand, unsatisfactory results were obtained due to an apparent and variable surface-state density when the second method was attempted. Unfortunately, there have been few experimental measurements on the grain boundary density of states in polycrystalline semiconductors.[36] Equation (10), which is used to describe the adsorption-reaction process, has been found to be "true" in the case of metal oxide semiconductors.[37] Further verification of its form in $BaTiO_3$, together with the assumption defined by Eq. (16), is desirable.

In a polycrystalline ensemble, such as ferroelectric (PTC) $BaTiO_3$, the nature of the elastic and electric boundary conditions upon the individual crystallites, is uncertain. The manner in which these conditions vary with temperature and time needs to be quantified, at least relative to a fixed temperature on the PTC anomaly curve, for reasons which are discussed below.

Owing to the observed large piezoresistivity coefficients in PTC barium titanate compositions,[17,38] the shape of the resistivity vs temperature curve is rather sensitive to changes in the elastic boundaries.[18,19] In addition, Samara[39] has shown that for both single and polycrystalline $BaTiO_3$ the Curie constant C decreases with hydrostatic pressure. The effects of a distributed Curie constant (due to inhomogeneous stresses) on the shape of the PTC anomaly have been discussed in Ref. 40.

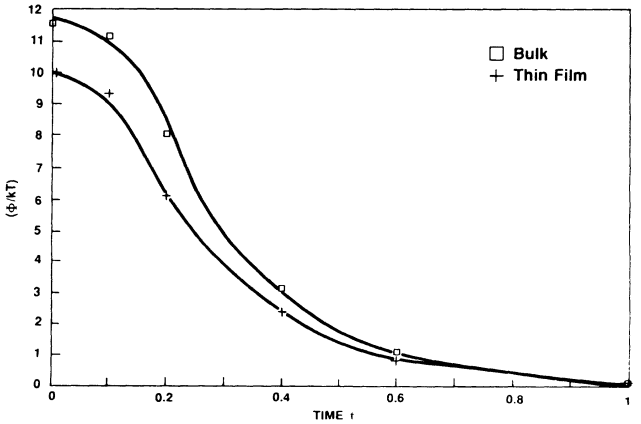

FIG. 13. Bulk and thin film transient response $(x/a=0.0)$.

In semiconducting-ferroelectric-semiconducting structures such as donor-doped PTC barium titanates, the ferroelectric properties of the grain boundary layer strongly control the electrical transport (below and above T_C). In addition to the semiconducting properties discussed earlier, a complete set of measurements of the ferroelectric properties of the grain boundary layer which are of interest for model computations is required. These properties include the electrostriction tensor components Q_{11} and Q_{12}: the extrapolated Curie-Weiss temperature T_0; and the Curie constant C. This type of measurement would be allowed on an insulating sample of the same composition, or on an excessively doped semiconducting sample to render it insulating.

[1]M. Kuwabara, Solid-State Electron., **27**, 929 (1984).
[2]M. Kuwabara and H. Inoue, Chem. Symp. Ser. **17**, 182 (1984).
[3]S. A. Gridnev, M. K. Chikanova, and S. P. Ostapenko, Izv. Akad. Nauk. SSSR, Neorg. Mater. **13**, 179 (1977).
[4]G. H. Jonker, Mater. Res. Bull. **2**, 401 (1967).
[5]O. Saburi, J. Phys. Soc. Jpn. **14**, 1159 (1959).
[6]W. Heywang, Solid-state Electron. **3**, 51 (1961).
[7]G. Goodman, J. Am. Ceram. Soc. **46**, 48 (1963).
[8]G. H. Jonker, Solid-State Electron. **7**, 895 (1964).
[9]B. M. Kulwicki, J. Phys. Chem. Solids **45**, 1015 (1984).
[10]A. Amin and R. E. Newnham, in *Electronic Ceramic Materials,* edited by J. Nowotny (Trans Tech, Aedermannsdorf, Switzerland, 1992).
[11]H. Ihrig and M. Klerk, Appl. Phys. Lett. **35**, 307 (1979).
[12]M. Khan, Ceram. Bull. **50**, 401 (1971).
[13]K. Daniels, H. Haerdtl, and R. Wernicke, Philips Tech. Rev. **38**, 73 (1978-79).
[14]G. V. Lewis, C. R. A. Catlow, and R. E. W. Casselton, J. Am. Ceram. Soc. **68**, 555 (1985).
[15]G. T. Malick, Jr. and P. R. Emtage, J. Appl. Phys. **39**, 3088 (1968).
[16]O. Saburi, J. Phys. Soc. Jpn. **14**, 1159 (1959).
[17]P. L. Janega, Solid-State Electron. **29**, 59 (1986).
[18]A. Amin, Phys. Rev. B **39**, 4350 (1989); **41**, 4784 (1990).
[19]A. Amin, Phys. Rev. B **40**, 11 603 (1989).
[20]J. Crank, *The Mathematics of Diffusion* (Clarendon, Oxford, 1975).
[21]H. S. Carslaw and J. C. Jaeger, *Conduction of Heat in Solids* (Oxford University Press, New York, 1959).
[22]F. M. Ryan and E. C. Subaro, Appl. Phys. Lett. **1**, 69 (1962).
[23]P. Gerthesen and K. Haerdtl, Z. Naturforsh. A **18**, 423 (1963).
[24]H. Ihrig and W. Puscfert, J. Appl. Phys. **48**, 3081 (1977).
[25]H. Ihrig, J. Phys. C **9**, 3469 (1976).
[26]H. Landolt and B. Börnstein, in *Ferroelectric and Antiferroelectric Substances,* edited by K. H. Hellwege, Landolt-Börnstein, New Series, Group III, Vol. 9 (Springer-Verlag, Berlin, 1975).
[27]*Ferroelectric Thin Films,* edited by E. R. Myers and A. I. Kingon, MRS Symposia Proceedings No. 200 (Materials Research Society, Pittsburgh, 1990).
[28]*Ferroelectric Thin Films II,* edited by A. I. Kingon, E. R. Myers, and B. Tuttle, MRS Symposia Proceedings No. 243 (Materials Research Society, Pittsburgh, 1992).
[29]*Ferroelectric Thin Films,* edited by A. S. Bhalla and K. M. Nair, Ceramic Transactions Vol. 25 (The American Ceramic Society, Westerville, Ohio, 1992).
[30]H. Kordi Ardakani, S. S. Shushtarian, S. M. Kanetakar, R. N. Karekar, and S. B. Ogale, J. Mater. Sci. Lett. **12**, 63 (1993).
[31]I. C. Noyana nd G. Sheikh, J. Matter. Res. **8**, 764 (1993).
[32]K. Kushida and H. Takeuchi, Appl. Phys. Lett. **50**, 1800 (1987).
[33]G. A. Rossetti, Jr., L. E. Cross, and K. Kushida, Appl. Phys. Lett. **59**, 2524 (1991).
[34]A. K. Goswami and L. E. Cross, Phys. Rev. **171**, 549 (1968).
[35]C. A. Miller, J. Phys. D **4**, 690 (1971).
[36]C. R. M. Groover, J. Phys. C **18**, 4079 (1985).
[37]J. W. Gardner, Semicond. Sci. Technol. **4**, 345 (1989).
[38]O. Saburi, J. Phys. Soc. Jpn. **15**, 733 (1960).
[39]G. A. Samara, Phys. Rev. **151**, 378 (1966).
[40]A. Amin, in *IEEE 7th International Symposium on Applications of Ferroelectrics,* edited by S. B. Krupandi and S. K. Kurtz (IEEE, Piscataway, NJ, 1990).